Angular emission characteristics of quantum cascade spiral microlasers

Martina Hentschel[1*], Tae-Yoon Kwon[1], Mikhail A. Belkin[2,3], Ross Audet[2,4], and Federico Capasso[2]

[1]*Max-Planck-Institut für Physik komplexer Systeme, Nöthnitzer Str. 38, D-01187 Dresden, Germany*

[2]*Harvard School of Engineering and Applied Sciences, Harvard University, Cambridge, Massachusetts 02138, USA*

[3]*Present address: Department of Electrical and Computer Engineering, University of Texas at Austin, Austin, TX 78712*

[4]*Present address: Edward L. Ginzton Laboratory, Stanford University, Stanford, CA 94305, USA*

[*]*Corresponding author: martina@pks.mpg.de*

Abstract: We perform ray and wave simulations of passive and active spiral-shaped optical microcavities, comparing our results to experimental data obtained with mid-infrared quantum cascade spiral microlasers. Focusing on the angular emission characteristics, we find that both ray and wave simulations are consistent with the experimental data, showing richly-featured, multidirectional far-field emission patterns in the case of uniform pumping and TM-polarized light. Active cavity simulations using the Schrödinger-Bloch model indicate that selective pumping of the quantum cascade spiral microlasers near the resonator boundary will yield unidirectional laser emission.

OCIS codes: (140.3945) Microcavities; (140.3410) Laser resonators; (140.1540) Chaos

References and links

1. G. D. Chern, H. E. Tureci, A. Douglas Stone, R. K. Chang, M. Kneissl, and N. M. Johnson, "Unidirectional lasing from InGaN multiple-quantum-well spiral-shaped micropillars," Appl. Phys. Lett. **83**, 1710-1712 (2003).
2. M. Kneissl, M. Teepe, N. Miyashita, N. M. Johnson, G. D. Chern, and R. K. Chang, "Current-injection spiral-shaped microcavity disk laser diodes with unidirectional emission," Appl. Phys. Lett. **84**, 2485-2487 (2004).
3. T. Ben-Messaoud and J. Zyss, "Unidirectional laser emission from polymer-based spiral microdisks," Appl. Phys. Lett. **86**, 241110 (2005).
4. A. Fujii, T. Nishimura, Y. Yoshida, K. Yoshino, and M. Ozaki, "Unidirectional laser emission from spiral microcavity utilizing conducting polymer," Jpn. J. Appl. Phys. **44**, L1091-L1093 (2005).
5. A. Tulek and Z. V. Vardeny, "Unidirectional laser emission from π-conjugated polymer microcavities with broken symmetry," Appl. Phys. Lett. **90**, 161106 (2007).
6. Ch.-M. Kim, J. Cho, J. Lee, S. Rim, S. H. Lee, K. R. Oh, and J. H. Kim, "Continuous wave operation of a spiral-shaped microcavity laser," Appl. Phys. Lett. **92**, 131110 (2008).
7. M. Hentschel and T.-Y. Kwon, "Designing and understanding directional emission from spiral microlasers," Opt. Lett. **34**, 163-165 (2009).
8. R. Audet, M. A. Belkin, J. A. Fan, B. G. Lee, K. Lin, and F. Capasso, "Single-mode laser action in quantum cascade lasers with spiral-shaped chaotic resonators," Appl. Phys. Lett. **91**, 131106 (2007).
9. A. Fujii, T. Takashima, N. Tsujimoto, T. Nakao, Y. Yoshida, and M. Ozaki, "Fabrication and unidirectional laser emission properties of asymmetric microdisks based on Poly(p-phenylenevinylene) Derivative," Jpn. J. Appl. Phys. **45**, L833-L866 (2006).
10. S.-Y. Lee, S. Rim, J.-W. Ryu, T.-Y. Kwon, M. Choi, and Ch.-M. Kim, "Quasiscarred Resonances in a Spiral-Shaped Microcavity," Phys. Rev. Lett. **93**, 164102 (2004).

#108170 - $15.00 USD Received 27 Feb 2009; revised 28 Apr 2009; accepted 10 May 2009; published 5 Jun 2009

11. S.-Y. Lee, S. Rim, J.-W. Ryu, T.-Y. Kwon, M. Choi and Ch.-M. Kim, "Ray and wave dynamical properties of a spiral-shaped dielectric microcavity," J. Phys. A **41**, 275102 (2008).
12. M. Hentschel and M. Vojta, "Multiple beam interference in a quadrupolar glass fiber," Opt. Lett. **26**, 1764-1766 (2001).
13. H. G. L. Schwefel, N. B. Rex, H. E. Tureci, R. K. Chang, A. D. Stone, T. Ben-Messaoud, and J. Zyss, "Dramatic shape sensitivity of directional emission patterns from similarly deformed cylindrical polymer lasers," J. Opt. Soc. Am. B **21**, 923-934 (2004).
14. S. Shinohara and T. Harayama, "Signature of ray chaos in quasibound wave functions for a stadium-shaped dielectric cavity," Phys. Rev. E **75**, 036216 (2007).
15. T. Tanaka, M. Hentschel, T. Fukushima, and T. Harayama, "Classical Phase Space Revealed by Coherent Light," Phys. Rev. Lett. **98**, 033902 (2007).
16. S.-B. Lee, J. Yang, S. Moon, J.-H. Lee, K. An, J.-B. Shim, H.-W. Lee, and S. W. Kim, "Universal output directionality of single modes in a deformed microcavity," Phys. Rev. A **75**, 011802 (2007).
17. M. Lebental, J. S. Lauret, J. Zyss, C. Schmit, and E. Bogomolny, "Directional emission of stadium-shaped microlasers," Phys. Rev. A **75**, 033806 (2007).
18. T. Harayama, S. Sunada, and K. Ikeda, "Theory of two-dimensional microcavity lasers," Phys. Rev. A **72**, 013803 (2005).
19. J. Wiersig and M. Hentschel, "Combining Directional Light Output and Ultralow Loss in Deformed Microdisks," Phys. Rev. Lett. **100**, 033901 (2008).
20. M. Hentschel and H. Schomerus, "Fresnel laws at curved dielectric interfaces of microresonators," Phys. Rev. E **65**, 045603(R) (2002).
21. H. Schomerus and M. Hentschel, "Correcting Ray Optics at Curved Dielectric Microresonator Interfaces: Phase-Space Unification of Fresnel Filtering and the Goos-Hänchen Shift," Phys. Rev. Lett. **96**, 243903 (2006).
22. S.-Y. Lee, J.-W. Ryu, T.-Y. Kwon, S. Rim, and C.-M. Kim, "Scarred resonances and steady probability distribution in a chaotic microcavity," Phys. Rev. A **72**, 061801(R) (2005).
23. C. Gmachl, E. E. Narimanov, F. Capasso, J. N. Baillargeon, and A. Y. Cho, "Kolmogorov-Arnold-Moser transition and laser action on scar modes in semiconductor diode lasers with deformed resonators," Opt. Lett. **27**, 824-826 (2002).
24. J. Wiersig, "Boundary element method for resonances in dielectric microcavities," J. Opt. A: Pure Appl. Opt. **5**, 53-60 (2003).
25. Note that they can be understood as normal scarred resonances in the framework of an amended ray optics where the Fresnel filtering and Goos-Hänchen corrections are included, see E. G. Altmann, G. Del Magno, and M. Hentschel, "Non-Hamiltonian dynamics in optical microcavities resulting from wave-inspired corrections to geometric optics," Europhys. Lett. **84**, 10008 (2008).
26. S. Rim, T.-Y. Kwon, J. Cho, and Ch.-M. Kim, "Quantal characteristics of a spiral shaped billiard," submitted to Phys. Rev. E.
27. T.-Y. Kwon, S.-Y. Lee, M. S. Kurdoglyan, S. Rim, Ch.-M. Kim, and Y.-J. Park, "Lasing modes in a spiral-shaped dielectric microcavity," Opt. Lett. **31**, 1250-1252 (2006).
28. The data is taken at a circle of radius $R = 3r_0$ and corresponds, strictly speaking, to the mid-field characteristics. The far-field profiles can be expected to be very similar to the data shown.
29. V. Moreau, M. Bahriz, J. Palomo, L. R. Wilson, A. B. Krysa, C. Sirtori, D. A. Austin, J. W. Cockburn, J. S. Roberts, and R. Colombelli, "Optical mode control of surface-plasmon quantum cascade lasers," IEEE Photon. Technol. Lett. **18**, 2499-2501 (2006).
30. V. Moreau, M. Bahriz, R. Colombelli, R. Perahia, O. Painter, L. R. Wilson, and A. B. Krysa, "Demonstration of air-guided quantum cascade lasers without top claddings," Opt. Express **15**, 14861-14869 (2007).
31. N. Hô, M. C. Phillips, H. Qiao, P. J. Allen, K. Krishnaswami, B. J. Riley, T. L. Myers, and N. C. Anheyer, Jr., "Single-mode low-loss chalcogenide glass waveguides for the mid-infrared," Opt. Lett. **31**, 1860-1862 (2006).
32. N. Tsujimoto, T. Takashima, T. Nakao, K. Masuyama, A. Fujii, and M. Ozaki, "Laser emission from spiral-shaped microdisc with waveguide of conducting polymer," J. Phys. D: Appl. Phys. **40**, 1669-1672 (2007).

1. Introduction

Microcavity lasers show great promise as low-threshold, single-mode lasers suitable for high-density integration. They are also fascinating to study as unique model systems combining problems from both quantum chaos and nonlinear laser physics. Spiral microcavity lasers have received particular attention in recent years. These devices have a top profile described in polar coordinates (r,ϕ) as $r(\phi) = r_0(1+\varepsilon-\varepsilon\phi/2\pi)$, as shown in Fig. 1(a), where ε is the deformation parameter. The devices possess a "notch" at $\phi = 0$ (2π), Fig. 1(a), which breaks the symmetry of the resonant cavity and potentially allows for unidirectional laser emission. To date, directional emission has been experimentally observed in a variety of spiral microlasers

#108170 - $15.00 USD Received 27 Feb 2009; revised 28 Apr 2009; accepted 10 May 2009; published 5 Jun 2009

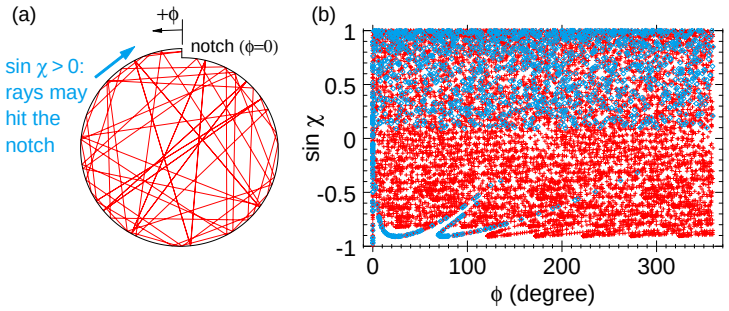

Fig. 1. (a) Spiral microcavity ($\varepsilon = 0.1$) with sample trajectory and (b) phase space portrait (red crosses). The blue diamond symbols mark a snapshot in the Poincaré SOS at the 4th bounce. See text for details.

operating in the ultraviolet, visible, and near-infrared wavelengths [1, 2, 3, 4, 5, 6]. The deformation parameter ε was between 0.1 and 0.2 in all these reports. Selective pumping near the outer boundary was found to improve the directionality [1, 2, 3, 6, 7], although directional emission was also reported for uniformly-pumped polymer-based spiral microlasers [4, 5].

Recently, quantum cascade (QC) spiral microlasers operating in the mid-infrared were reported [8]. Emission from these devices is not unidirectional; instead, the far-field measurements (Fig. 2) show complex profiles with multiple peaks in emission intensity. There are some notable differences between the QC spiral lasers and the other spiral microlasers mentioned previously [1, 2, 4, 5, 3, 6, 7] that may explain the significant qualitative differences in the far-field profiles. First, the ratio of cavity size to the wavelength in the material ($r_0/\lambda_n \approx 15-50$) for the QC devices in Ref. [8] is by far the smallest of all the spiral microlasers cited above. Second, QC lasers are intrinsically TM-polarized devices. Finally, unlike most of the spiral microlasers, the QC lasers were uniformly injection-pumped [8]. To better understand how these factors may affect the emission profiles, it is helpful to perform a variety of simulations.

The goal of this work is to provide a consistent picture of emission from QC spiral microlasers in a manner that explains experimentally observed far-field profiles. This is accomplished by both ray and wave simulations, focusing on TM-polarized spiral microlasers with small cavity size to wavelength ratio.

2. Ray simulations

The multitude of experimental demonstrations of spiral microlasers [1, 2, 3, 4, 5, 6, 7, 8] is contrasted by a relative lack of theoretical investigations of the emission characteristics of spiral microcavities, using either the wave [1, 9] or ray approaches. In particular, there are very few ray simulations reported in the literature [10, 11], and these existing reports do not concern the far-field properties. This is surprising, given the many successes of the ray model in describing the emission properties of microcavities [12, 13, 14], even in the lasing case [15, 16, 17].

Here, we demonstrate that ray simulations are a useful and versatile tool for predicting the angular emission properties of spiral microcavities. We simulate the far-field profiles of spiral microlasers with TM-polarized laser modes (as is the case for QC lasers) using ray simulations of spiral Fresnel billiards [12, 13, 14]. The advantage of ray simulations over wave calculations is their greater computational efficiency, which allows one to make predictions with extremely low numerical effort. A sample trajectory and the corresponding phase space in the form of a Poincaré surface of section (SOS), taken at the cavity boundary for the spiral resonator with $\varepsilon = 0.1$, $r_0 = 1$, are shown in Figs. 1(a) and (b), respectively. The Poincaré SOS was obtained

#108170 - $15.00 USD Received 27 Feb 2009; revised 28 Apr 2009; accepted 10 May 2009; published 5 Jun 2009

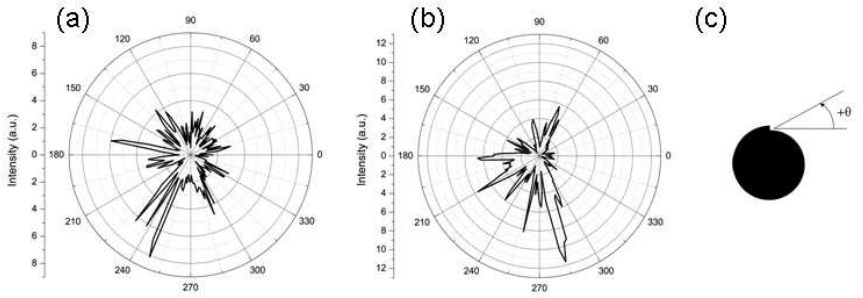

Fig. 2. Far-field profile measured for a quantum cascade spiral microlaser with (a) $r_0 = 80\mu$m and $\varepsilon = 0.125$ and (b) $r_0 = 110\mu$m and $\varepsilon = 0.091$. The lasers were operated above threshold in pulsed mode at room temperature. Zero angle is defined as perpendicular to the spiral notch as shown in (c).

by starting 170 test rays in a clockwise direction with random initial conditions and then following them over 20 bounces (shown as red crosses). There are no islands of stability visible in Fig. 1(b). In contrast to disk resonators, angular momentum is not conserved in the spiral resonators because of the non-constant (decreasing or increasing, depending on the sense of rotation) radius of curvature.

All rays started in the clockwise direction ($\sin\chi > 0$) will eventually hit the notch and thereby change their sense of rotation to counter-clockwise ($\sin\chi < 0$). The blue diamond symbols in Fig. 1(b), which present a snapshot of the test rays taken at the fourth bounce, illustrate how this happens. By the fourth bounce, most of the rays that started in the clockwise direction have not yet hit the notch; hence, coverage of the upper half ($\sin\chi > 0$) of the Poincaré SOS is essentially uniform. Rays that hit the notch on one of the first four bounces have changed their sense of rotation to counter-clockwise ($\sin\chi < 0$) and correspond to the blue, nearly connected, curved signatures (called "tentacle structures" in Ref. [10]) in the lower half of Fig. 1(b). As the notch is located at $\phi = 0$, the vertical signature in the Poincaré SOS at this position indicates the route to counter-clockwise rotation: the position angle ϕ for all the rays hitting the notch is zero and the angles of incidence χ vary.

The tentacle-type signatures that consist of blue diamonds in the lower half of Fig. 1(b) ($\sin\chi$ close to -1) correspond to the next bounces (up to 3) of the rays that hit the notch at $\phi = 0$ and change their sense of rotation. These trajectories typically hit the boundary under a rather large angle $|\chi|$. The distinct structure in phase space is formed because the small spatial extent of the notch defines a limited set of initial conditions associated with hitting the notch. The tentacle signatures blur over the next few bounces, but can still be recognized as such before the chaotic character of the resonator dominates the long-time dynamics.

The simulations of the far-field profiles for spiral resonators with various deformation parameters ε are obtained by complementing the ray dynamics with Fresnel's law [12, 13, 14, 15, 19], and constructing the far field from a large number of test rays (10^5) whose intensity develops according to Fresnel's law for TM-polarized light. The intensity and far-field directionality of escaping light rays is collected in bins of one degree, and subsequently smoothed over a two-degree window that mimics a finite detector resolution in experiments. The convincing agreement found previously between ray simulated far-field patterns and those obtained in experiments with other uniformly pumped microlasers (cf., e.g., Ref. [15]) suggests that starting test rays with random initial conditions effectively simulates, and adequately describes, the

#108170 - $15.00 USD Received 27 Feb 2009; revised 28 Apr 2009; accepted 10 May 2009; published 5 Jun 2009

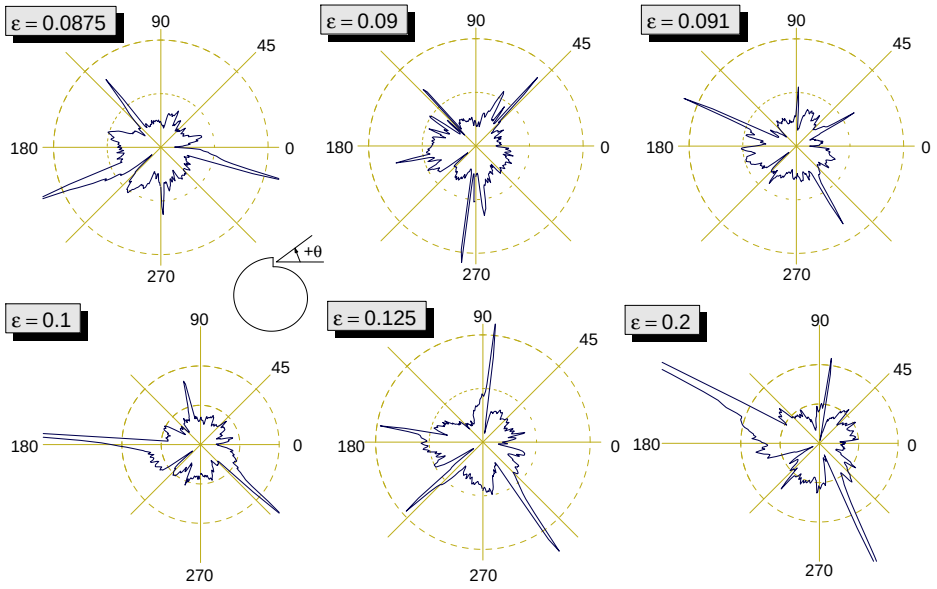

Fig. 3. Far-field patterns based on the ray picture for TM-polarized light and various geometries similar to those in Ref. [8]. The far-field angle θ is measured with respect to the notch ($\theta = 0$ meaning emission perpendicular to the notch surface, see inset). 10^5 rays are started with random initial conditions and data is taken from the steady probability distribution. Intensity is in arbitrary units.

uniformly pumped case. We therefore expect good qualitative agreement between our ray simulations and the experimental results obtained for the uniformly pumped QC lasers used in Ref. [8].

In accordance with the experiments in Ref. [8], we assume a cavity refractive index of $n = 3.15$. The curvature of the cavity boundary would formally require the use of adjusted Fresnel's laws [20, 21]; however, for the intermediate size parameters $\mathrm{Re}(nkr_0)$ realized in the experiment [8] (and because our results rest on the steady probability distribution, [22]) the use of the planar-interface Fresnel formulas is justified.

The ray-simulated far-field profiles for TM-polarized laser light are shown in Fig. 3. We measure the far-field angle θ with respect to the notch (cf. Fig. 3, inset), noting it is distinct from the polar angle ϕ along the cavity boundary. The simulation results for TM-polarized modes qualitatively resemble the experimental findings reported in Ref. [8] and shown in Fig. 2. In particular, both simulation and experiment reveal that on a more or less uniform background, a small number of emission directions are preferred. The corresponding far-field angle θ of these emission peaks are highly sensitive to the deformation parameter ε of the spiral. This implies that small processing imperfections may result in large differences in the far-field profiles of QC spiral microlasers of identical size and shape, as has been observed experimentally. Furthermore, there is no observable relation between the position of the peaks and the location of the notch. Both of these facts reflect the chaotic dynamics of the spiral cavity, as illustrated in Fig. 1.

Ray simulations of the far-field for TE-polarized light were also performed (not shown here). The simulations show improved directionality relative to TM-polarized light, in agreement with results for other microcavity geometries [23, 19]. The underlying mechanism is the existence of the Brewster angle, which singles out one or two spikes as preferred far-field emission char-

#108170 - $15.00 USD Received 27 Feb 2009; revised 28 Apr 2009; accepted 10 May 2009; published 5 Jun 2009

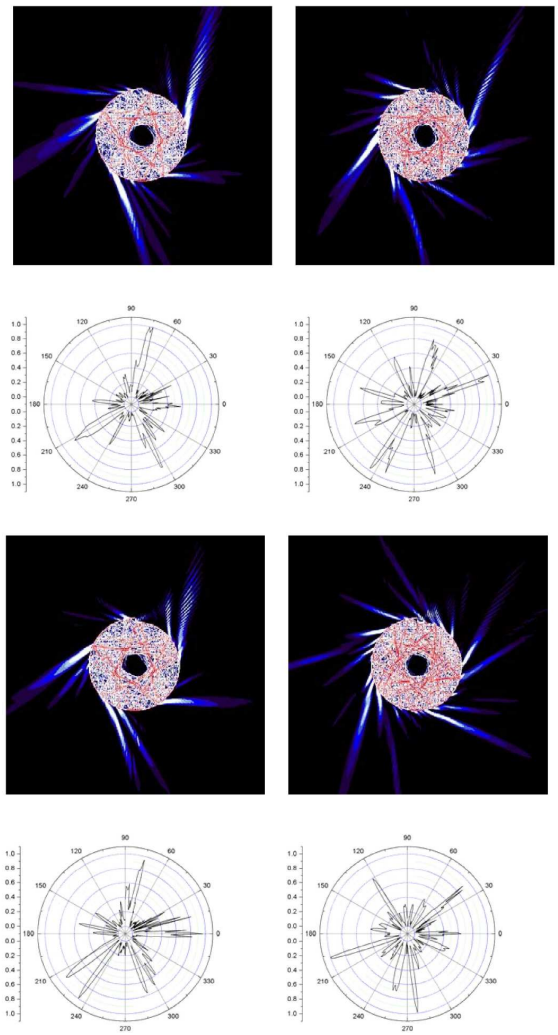

Fig. 4. Wave and far-field patterns (upper and lower panels, respectively) of four neighboring resonances of the passive cavity with comparable *Q*-factors around 4400 and wavenumbers near 1430 cm^{-1} . The presence of the notch does not affect the emission patterns in any obvious way, and the radiation emerges in multiple directions that also depend on the resonance chosen. The existence of a number of emission directions on an appreciable background makes these far-field profiles qualitatively similar to those experimentally observed and ray-simulated.

acteristics. Evidence of improved directionality for TE-polarized light provides a partial explanation of why the profiles of other spiral microlasers, such as in Refs. [4, 5], may show greater directionality than the QC microlasers. Because QC lasers cannot emit TE light, other techniques such as boundary pumping must be employed in QC spiral lasers to achieve directional emission. This will be discussed later in the paper.

#108170 - $15.00 USD Received 27 Feb 2009; revised 28 Apr 2009; accepted 10 May 2009; published 5 Jun 2009

3. Wave simulations

To further explore the far-field emission profiles of spiral microcavities, the resonance spectrum is simulated using the boundary element method (BEM) [24]. We concentrate on cavity modes with a high Q-factor near wavenumbers 1430 cm^{-1} (corresponding to the peak of the laser gain in Ref. [8]), as these modes will have the lowest lasing threshold and, consequently, can be expected to be the lasing modes near threshold.

The wave patterns and the corresponding far-field emission profiles are shown in the upper and lower parts, respectively, of Fig. 4. Here, one sees that the intensity spikes pointing in various emission directions originate at certain positions along the cavity boundary. They are directly related to the internal mode structure and leave the cavity in the counter-clockwise direction. Although this is a consequence of the presence of the notch, no obvious relationship exists between the far-field intensity maxima and the position of the notch.

Comparing these results with the ray simulations and the experimental data, cf. Figs. 2, 3, and 4, there is convincing qualitative agreement. Specifically, the far-field profiles are not unidirectional. They are strongly non-isotropic, with a series of observed sharp peaks. The position of the peaks has no clear relationship to the position of the notch. This contrasts with the far-field profiles of the non-QC spiral microlasers [4, 5].

A closer investigation of the resonant wave patterns shown in Fig. 4 reveals no obvious signs of regularity that would allow one to easily classify them, for example, as whispering gallery modes (WGMs). This should not be surprising, however, because angular momentum is not conserved. Previously, regular mode structures have been seen in numerical simulations for spiral cavities with refractive indices of $n=2$ and $n=3$ (the latter being close to the value used here). The mode structures were termed quasi-scarred resonances [25] and possessed triangular and star-like shapes, respectively [10, 11]. This type of resonance is distinctly different from the resonances found in spiral billiards, [26] which correspond to the cavity in the limit $n \to \infty$. Modes similar to the quasi-scarred modes in [10] do indeed play a role in the present case, as can be seen from the wave patterns in Fig. 4 – elements of star-type, triangular, and more complicated compound patterns can be identified. However, that there is no distinct pattern present in the internal mode structures that would give rise to predictable far-field characteristics. This is in agreement with the experimental observations.

We close this section by discussing the role of diffraction, which should be considered because the spiral notch and the neighboring sharp corners are features whose size is on the order of the wavelength. Diffraction from the sharp corners was suggested as the cause of directional emission from the spiral microlasers in Ref. [1]. Realizing that diffraction effects are naturally included in the wave simulations and experiments but missing in ray-based simulations, the agreement between the far-field patterns in all three approaches is surprising, and would suggest that diffraction is dominated by other effects.

4. Uniform vs. boundary pumping

We have seen in the previous sections that unidirectional light output is not expected from uniformly pumped, TM-polarized QC lasers of spiral shape. While uniform pumping was used in the QC laser experiments [8], most of the other experimental studies that demonstrated directional emission [1, 2, 3, 6] utilized so-called boundary pumping, in which only the perimeter of the resonator was pumped. We shall now see that this crucially influences the far-field profile of the devices.

To this end, we have performed simulations of spiral microlasers with active material in the framework of the Schrödinger-Bloch model [18]. Note that ray simulations fail to capture the radiation characteristics in the case of non-uniform pumping, as do wave simulations based on passive resonator cavities such as used in Ref. [1]. We have used a size parameter $\mathrm{Re}(nkr_0) \approx$

#108170 - $15.00 USD Received 27 Feb 2009; revised 28 Apr 2009; accepted 10 May 2009; published 5 Jun 2009

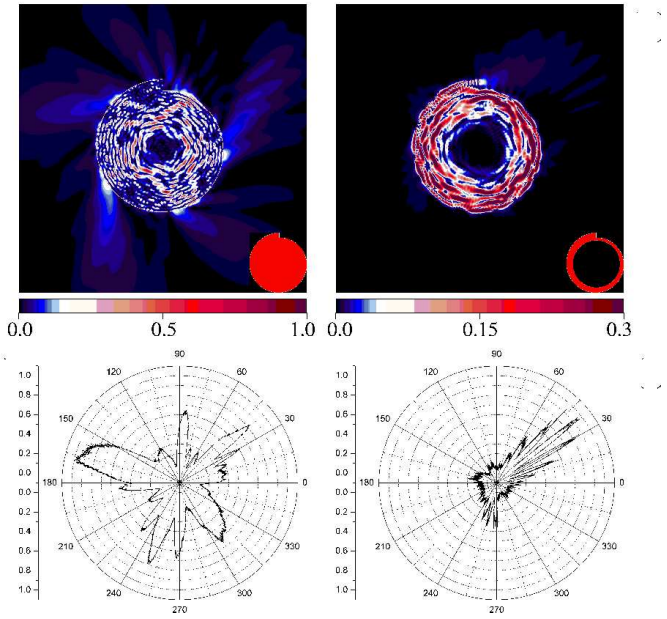

Fig. 5. Uniform (left panels) and boundary (right panels) pumping of spiral-shaped microlasers [$\mathrm{Re}(nkr_0) \approx 62, \varepsilon = 0.2, n = 3.15$]. The area pumped is shown in the insets; in the case of selective pumping the boundary area pumped is at least $0.1r_0$. The upper panels show snapshots of the intensity distribution in the lasing cavity. The internal mode dynamics often lead to a pulsed light output [7]. The lower panels show the far-field patterns (for the pumping strength $w = 0.0002$, slightly above the lasing threshold) as a function of angle. The uniformly pumped device (left) has multidirectional laser emission, whereas the boundary-pumped device (right) has highly directional emission.

62, which is smaller than the devices used in the experiments [8]. This choice was motivated by the strongly increasing numerical cost of simulations with larger size parameters. We have adjusted the notch size to $\varepsilon = 0.2$, which makes the physical size of the notch (and therefore its effect) similar to that used in Ref. [8].

Our results are summarized in Fig. 5 (see also Ref. [7] for a more general discussion of the problem). In the left panels, the entire resonator area is pumped, whereas in the right panels, only the region close to the boundary is pumped [27]. The pumped areas are indicated in the insets. The upper panels show a snapshot of the intensity distribution inside and outside the lasing cavity. The far-field profiles [28] are shown in the lower panels. For the case of uniform pumping, multi-directional emission is observed, confirming our previous findings from passive cavity simulations, and providing further evidence of the usefulness of passive cavity simulations for predicting the near-threshold behavior of uniformly pumped devices. For the case of boundary pumping, directional emission is clearly visible. The light is emitted at angle of $\theta \approx 40^\circ$, which is consistent with other experimental results [1, 2, 3, 6].

The results presented in Fig. 5 thus indicate that one can achieve directional emission with quantum cascade spiral microlasers that are injection-pumped along the boundary of the resonator. We note that it should be possible to achieve boundary pumping in QC spiral microlasers by selectively patterning narrow electrical contacts along the outer portion of the spiral surface. Lateral current spreading in a typical QC device is limited to $< 25\mu$m [29, 30], and hence the central region of a spiral micropillar with radius $r_0 \approx 100\mu$m will remain unpumped, enabling

#108170 - $15.00 USD Received 27 Feb 2009; revised 28 Apr 2009; accepted 10 May 2009; published 5 Jun 2009

directional emission. A detailed theoretical and experimental investigation of this conjecture will be the subject of further study.

5. Summary

We have performed ray and wave simulations of spiral microcavities, motivated by recent experiments involving uniformly-pumped, TM-polarized quantum cascade spiral microlasers emitting in the mid-infrared [8]. The simulated far-field profiles are consistent with the experimental results of Ref. [8], with all showing a number of sharp peaks in the far-field emission, located at angles that depend sensitively on the deformation parameter ε. The qualitative agreement between the ray and wave simulations suggests that ray simulations can be of great utility for understanding uniformly-pumped spiral lasers, because they are significantly faster to compute than wave simulations.

In an effort to improve the far-field directionality, we considered boundary pumping of the QC spiral microlasers. Passive cavity simulation techniques become invalid in the case of non-uniform pumping, so the Schrödinger-Bloch framework was used. The Schrödinger-Bloch simulations indicate that unidirectional emission from QC spiral microlasers can be attained by selectively injecting current near the resonator boundary. Future experimental and theoretical work will focus on achieving optimized unidirectional emission from the notch of the QC spiral microlasers. This would enable directional emission into free space as well as the possibility of coupling the emitted light into a chalcogenide fiber or waveguide [31] positioned at the notch of the spiral [32].

Acknowledgments

We would like to thank Eric Heller for initially drawing our attention to this field. M.H. thanks the German Research Foundation (DFG) for support within the Emmy-Noether Programme and the Research Unit FG 760. T.-Y.K. was supported in part by the "Korea Research Foundation (KRF) Grant" funded by the Korean government (MOEHRD) under contract number KRF-2006-352-C00022. M.B. and F.C. acknowledge financial support from the Air Force Office of Scientific Research under contract number FA9550-08-1-0047.

#108170 - $15.00 USD Received 27 Feb 2009; revised 28 Apr 2009; accepted 10 May 2009; published 5 Jun 2009